UPCommons

Portal del coneixement obert de la UPC

http://upcommons.upc.edu/e-prints

Article publicat */ Published paper*:

Arrayago, I.; Real, E., Mirambell, E. (2015). Experimental study on ferritic stainless steel RHS and SHS beam-columns. Thin-walled structures, 100. 93-104. Doi: 10.1016/j.tws.2015.12.004

Experimental study on ferritic stainless steel RHS and SHS beam-columns

I. Arrayago*, E. Real, E. Mirambell

Department of Civil and Environmental Engineering, Universitat Politècnica de Catalunya – BarcelonaTech, Barcelona, Spain

*Corresponding author: Tel: +34 934054156; Fax: +34 934054135, e-mail: itsaso.arrayago@upc.edu

ABSTRACT

Ferritic stainless steels, with their lower nickel content, supplement the desirable features offered by different stainless steel grades with a more controlled and lower initial investment requirements, which have encouraged the use of these materials in construction. The nonlinear behaviour of stainless steel grades is not usually considered when extending design expressions codified for carbon steel to these alloyed materials, leading to overconservative design approaches and the applicability of the different design expressions initially developed for carbon steel needs to be adjusted for every stainless steel grade. The study of stainless steel elements subjected to combined flexural buckling and bending moment loading conditions only covers the most usual austenitic, duplex and lean duplex grades, but experimental results on ferritic grades are still necessary to complete the analysis. Hence, an experimental programme on ferritic stainless steel RHS and SHS pin-ended elements has been conducted where the flexural buckling and beam-column behaviour of these elements has been investigated. Furthermore, the assessment of the different design approaches for flexural buckling and interaction expressions for combined loading has been derived from the obtained experimental results, and current specifications provided in Standards have been found to be, in general, safe but overconservative.

HIGHLIGHTS

- Experimental programme on ferritic stainless steel RHS and SHS elements is presented.

- Flexural buckling resistance of pin-ended columns is investigated.

- Design expressions for flexural buckling resistance predictions are assessed.

- Beam-column behaviour of pin-ended columns under uniform bending is studied.

- Codified and alternative interaction expressions for beam-columns are assessed.

KEYWORDS

beam-columns, cold-formed, experimental program, ferritic stainless steel, flexural buckling, hollow sections, interaction expressions

1. INTRODUCTION

The utilization of stainless steel alloys as structural elements has been increased in the last few years, mostly caused by their excellent corrosion resistance, easy maintenance, aesthetic appearance and appropriate mechanical properties. However, the utilization of these materials is still restrained by the need of high initial investment related to stainless steels. Hence, stainless steel producers have been hardly working on the development of new grades, such as ferritics, which are reasonably cheaper and more price-stable than the most usual austenitic grades due to their lower nickel content, while maintaining a significant corrosion resistance, good ductility, formability and impact resistance.

Despite the different stress-strain behaviour and the considerable strain hardening presented by stainless steel alloys, guidance for structural stainless steel elements EN1993-1-4 [1] is usually based on the specifications for carbon steel gathered in EN1993-1-1 [2], being in general too conservative. Thus, the development of specific and efficient guidance is key to the generalization of these alloyed materials.

Concerning the behaviour of stainless steel columns, the study has been mainly focused on the most usual austenitic and duplex grades. Some recent tests on austenitic [3], duplex [4] and

lean duplex [5] elements subjected to combined axial compression and bending moment loading conditions are available in the literature in addition to flexural buckling investigations. However, experimental results on ferritic stainless steel are limited, especially regarding Rectangular and Square Hollow Section (RHS and SHS) elements: a single experimental programme on RHS and SHS columns subjected to pure compression was reported by [6] although no beam-column tests have been published as far as the authors know. The behaviour of beam-columns has been, nevertheless, numerically investigated for the different grades. Therefore, design specifications codified in different Standards (such as European EN1993-1-4 [1], North American SEI/ASCE-8 [7] and Australian AS/NZS [8] Standards) for the consideration of the interaction expressions for beam-columns of ferritic stainless steel columns still need to be experimentally studied and validated.

Additionally, a re-evaluation of the partial safety factors for the design of stainless steel elements has been recently published by Afshan et al. [9], where an extensive experimental database is statistically analysed according to Annex D of EN1990 [10]. The results highlight that a potential problem exists for ferritic and duplex RHS members in compression, where a safety factor of γ_{M1}=1.2 would appear to be more appropriate in contrast to the value codified in EN1993-1-4 [1], γ_{M1}=1.1. Given the number of available test data, this could also be an indication that the buckling curve is too high. Some similar conclusions have also been published by Arrayago et al. [11] after conducting a numerical analysis in ferritic stainless steel RHS and SHS beam-columns, where the currently codified safety factor γ_{M1} has been found to be unsafe for some of the analysed specimens.

In order to complete this research, a comprehensive experimental programme on ferritic stainless steel RHS and SHS beam-columns was conducted, where five different RHS and SHS elements subjected to concentric and eccentric axial compression were analysed. These

elements were tested under pin-ended conditions and regarding RHS, minor axis buckling was considered. The assessment of different design approaches has been derived from the experimental results for flexural buckling and combined loading, and they will be used for the validation of the finite element models in future numerical analysis of the phenomena.

2. EXPERIMENTAL TESTS

2.1 Introduction

This paper presents a comprehensive experimental programme conducted in the Laboratori de Tecnologia d'Estructures Luis Agulló, in the Department of Construction Engineering at Universitat Politècnica de Catalunya, where the flexural buckling and beam-column response of ferritic stainless steel RHS and SHS members was analysed. The studied ferritic grade was EN1.4003 and five different cross-sections, consisting of two SHS and three RHS were tested. These cross-sections were labelled as follows: S1-80x80x4, S2-60x60x3, S3-80x40x4, S4-120x80x3, S5-70x50x2 and this nomenclature has been assumed throughout the paper.

2.2 Material, geometric and initial imperfection characterization

Any relevant information regarding the specimens to be tested was accurately measured and acquired before testing in order to correctly analyse the experimental results. Thus, the actual material behaviour, geometrical definition and initial imperfections were carefully defined.

The mechanical behaviour of the different cross-sections was determined by conducting several tensile tests on coupons extracted from similar specimens to those to be tested, where coupons from both flat (F) and corner (C) parts of the specimens were tested. This allowed for the evaluation of the cold-forming effects, which led into an increase in both the proof stress $\sigma_{0.2}$ and the ultimate tensile strength σ_u, while ductility was considerably reduced. Since the experimental programme described in this paper was part of a more general experimental

4

programme, where different ultimate responses of ferritic stainless steel RHS and SHS elements were investigated, the more in detail aspects of the material behaviour of the analysed specimens has already been published in [12,13]. Therefore, a summary of the most relevant information regarding tensile coupon testing is described in this section.

All coupons were tested in accordance with the specifications in ISO6892-1 [14] and the mechanization of the coupons and the execution of the tensile tests were performed in Acerinox (see Figure 1). The key material parameters were then determined from the measured stress-strain data through a software that directly provides parameter values, and which has been described in Real et al. [15] and Arrayago et al. [16]. The average values of these parameters for the flat and corner coupons of each cross-section are summarized in Table 1, where E is the Young's modulus, $\sigma_{0.05}$ and $\sigma_{0.2}$ are the proof stresses corresponding to 0.05% and 0.2% plastic strains respectively, σ_u is the ultimate tensile strength, ε_u is the corresponding ultimate strain and ε_f is the strain at fracture measured over the standard gauge length of $5.65\sqrt{A_c}$ where A_c is the cross-sectional area of the coupon. Strain hardening exponents n and m corresponding to the material model proposed by Mirambell and Real [17] are also reported.

Table 1. Average material properties from coupon tensile tests.

	E [MPa]	$\sigma_{0.05}$ [MPa]	$\sigma_{0.2}$ [MPa]	σ_u [MPa]	ε_u [%]	ε_f [%]	n	m
S1 – F	173992	467	521	559	8.2	21.7	12.4	2.3
S1 – C	170049	441	577	645	1.1	7.9	5.0	5.4
S2 – F	186896	433	485	505	6.8	20.9	12.2	2.6
S2 – C	178049	459	555	587	1.0	10.1	7.9	5.2
S3 – F	181632	467	507	520	3.6	21.0	16.4	2.5
S3 – C	183684	434	558	601	1.0	7.0	5.9	4.5
S4 – F	176704	391	430	490	12.6	27.1	14.6	2.3
S4 – C	194611	457	540	583	1.0	10.1	7.6	4.8
S5 – F	179568	381	418	480	13.8	26.8	15.3	2.4
S5 – C	186026	466	552	575	1.1	6.5	8.0	4.6

<div style="text-align:center">
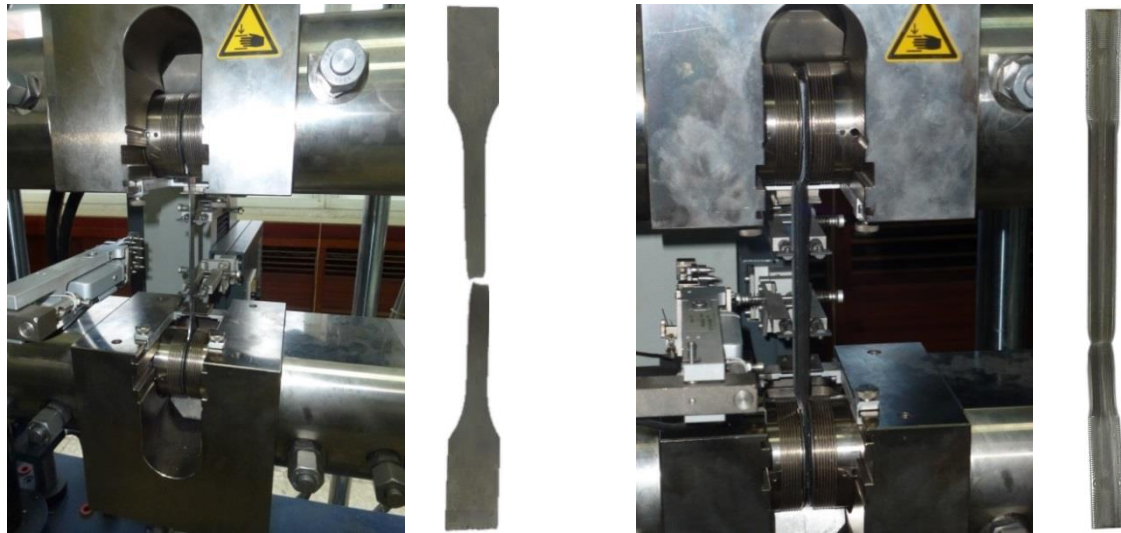
(a) Testing of S3-F coupon and tested flat coupon   (b) Testing of S2-C coupon and tested corner coupon

Figure 1. Tensile coupon tests on flat and corner coupons respectively.

</div>

However, for the analysis of experimental tests and the assessment of different predicting expressions the weighted average material properties are usually determined [6,12,13,18] from coupon tests, calculating the weights according to the area of the flat/corner parts referred to the total area of the cross-section. Weighted average material parameters are presented in Table 2 and will be used throughout the different analyses in this paper.

<div style="text-align:center">

Table 2. Weighted average material properties.

</div>

	E [MPa]	$\sigma_{0.05}$ [MPa]	$\sigma_{0.2}$ [MPa]	σ_u [MPa]	ε_u [%]	n	m
S1	172615	456	539	587	5.8	8.8	2.6
S2	183667	442	509	533	4.8	11.0	3.2
S3	182637	451	529	554	2.5	12.9	2.7
S4	188482	406	453	509	10.0	13.8	2.6
S5	181030	400	449	502	10.8	14.7	2.4

The actual geometry of all specimens was carefully determined by the measurement of all the relevant dimensions, which are summarized in Table 3. L is the total length of the specimens, H is the total height, B is the total width, t is the thickness and R_{ext} is the external corner radius, as defined in Figure 2. For every cross-section, a flexural buckling (i.e. concentric compression) test, named CC, was conducted, together with one or two beam-column (i.e. eccentric compression) tests, named EC1 and EC2 respectively.

Table 3. Measured dimensions for the tested specimens.

Specimen	L [mm]	H [mm]	B [mm]	t [mm]	R_{ext} [mm]	w_0 [mm]
S1-CC	1495	79.6	80.2	3.9	7.0	0.81
S1-EC1	1495	80.1	80.3	3.9	7.3	1.25
S1-EC2	1498	79.9	80.3	4.0	7.5	1.38
S2-CC	1500	60.3	60.2	2.9	5.9	0.66
S2-EC1	1500	60.0	60.2	3.0	5.9	0.69
S3-CC	1500	80.0	40.0	3.8	6.8	0.85
S3-EC1	1500	80.0	40.2	3.8	6.5	0.89
S4-CC	1500	119.8	79.8	2.9	7.2	1.21
S4-EC1	1500	119.8	79.6	3.0	7.2	1.58
S5-CC	1500	70.0	49.6	2.0	4.4	1.09
S5-EC1	1500	70.0	49.9	2.0	4.2	1.32
S5-EC2	1500	70.1	49.9	2.0	4.3	1.35
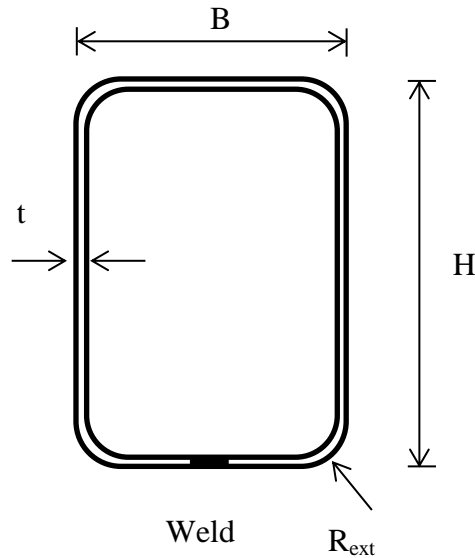
Figure 2. Definition of cross-section symbols.

Since the experimental programme presented in this paper consists of flexural buckling tests, initial global imperfections are an important aspect to be considered in order to define the adequate position of each specimen during the tests and validate future finite element models. Thus, the magnitude and distribution of the initial bow of each specimen was carefully measured by a laser device. Columns were supported onto two fixed points at both ends and the imperfections were measured by moving the laser device over a completely horizontal surface, recording measurements every 100mm and at mid-height section, as shown in Figure 3. The maximum global imperfection amplitude w_0 of each specimen is presented in Table 3.
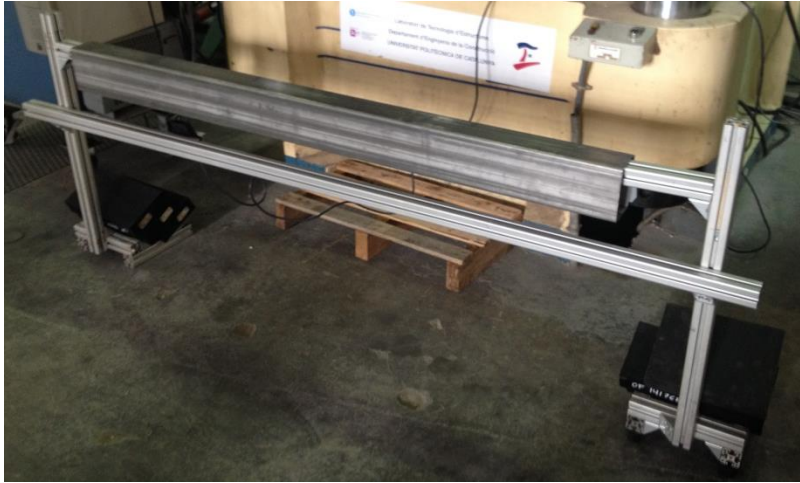
Figure 3. Set-up for global initial imperfection measurement.

2.3 Flexural buckling and beam-column tests

Flexural buckling and beam-column tests on ferritic stainless steel elements were conducted in order to investigate their buckling behaviour and assess the expressions currently specified in Standards and proposed in the literature, as well as the adequacy of the current safety partial factor γ_{M1}. Therefore, five ferritic RHS and SHS elements with a nominal length of 1500mm were tested under pure compression and combined axial compression and bending moment loading conditions, with pin-ended ends. For those RHS involved in the study, minor axis buckling was considered.

The general test set-up of flexural buckling tests is presented in Figures 4 and 5, where the most relevant elements are indicated, together with a photograph of S1-CC specimen prior to testing. Pin-ended conditions were guaranteed by two pin-ended bearings, which allowed free rotations about minor axis and fixed conditions about the orthogonal axis, as presented in Figure 6. These bearings were specially mechanized and consisted on a plate with a knife edged wedge and a plate containing a V-shaped pit. The lower pit plate was connected to an end support, while the upper one was connected to the hydraulic jack. Two steel end plates were welded to each specimen at both extremes, at a specified eccentricity, and the end plates were bolted to the wedged plates.
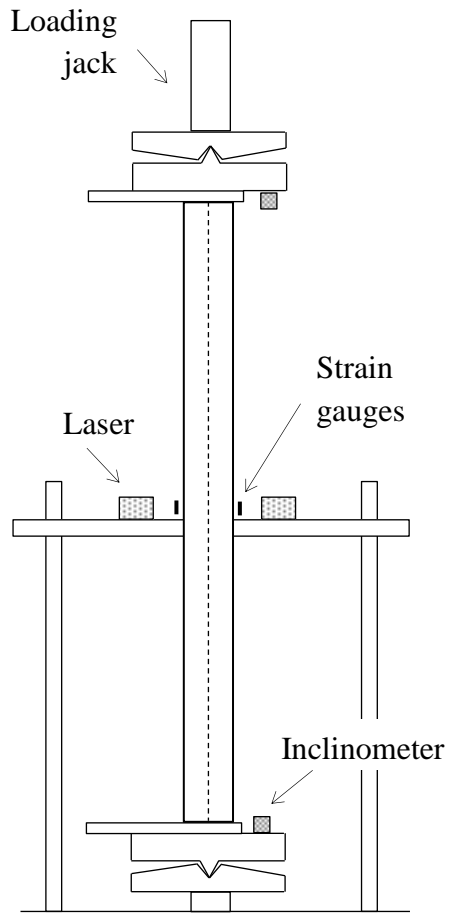
Figure 4. Schematic diagram of the test setup for flexural buckling and beam-column tests.

Figure 5. S1-CC specimen prior to testing.
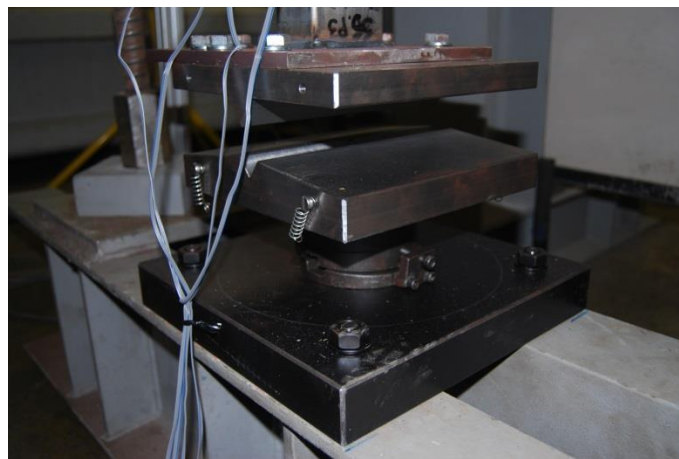
Figure 6. Lower pin-ended bearing.

Although the nominal length L of each specimen was 1500mm, the effective length of the system L_e equal to the distance between knife-edges will be considered in further analysis.

Hence, the thickness of both end plates and the bearing plates need to be added to the length of the specimens, which leads into L_e=1600mm. Thus, the member slenderness $\overline{\lambda}$ spectrum of the specimens ranged from 0.65 to 1.72, calculated according to EN1993-1-4 [1], Eq. (1).

$$\overline{\lambda} = \sqrt{\frac{A\sigma_{0.2}}{N_{cr}}} \tag{1}$$

where A is the cross-sectional area (effective area has been considered for Class 4 cross-sections), $\sigma_{0.2}$ is the 0.2% proof stress and N_{cr} is the Euler elastic critical load for flexural buckling.

Regarding the testing procedure, the specimens, together with the bolted edge plates, were placed into the machine and the actuator was then slowly moved closer until they were in contact. To ensure full contact and avoid settlement effects, a compression load of 3kN was applied, which was negligible compared to the achieved ultimate loads. The tests were then conducted under displacement control at a testing rate of 0.2mm/min, in order to reduce any possible dynamic effect, and allowing the test to continue to the post-ultimate stage.

The instrumentation of the specimens consisted of two laser devices measuring the lateral horizontal deflections about the minor axis at mid-height, two inclinometers on the welded steel plates measuring end rotations and string potentiometers determining end shortenings, as shown in Figures 4-7. The applied load was directly measured from the loading machine. Four linear electrical resistance strain-gauges were affixed to the extreme tensile and compressive fibres of the mid-height sections in the axial direction, at a distance of four times the material thickness from the corners, to capture longitudinal strains and the determination of the actual initial loading eccentricities. All the information was recorded by an MGCPlus data acquisition system at $2s^{-1}$ intervals.

Figure 7. In detail instrumentation setup at mid-height section.

2.4 Experimental results

Experimental results on ferritic RHS and SHS elements tested under pure compression and combined loading are presented in this section. Key experimental aspects are summarized in Table 4, where N_u is the ultimate compression load, M_u is the bending moment when N_u is reached, d_u and θ_u are the lateral deflection and the total rotation corresponding to N_u respectively. M_u represents the total bending moment, comprising the first order bending moment due to load eccentricity e_0 ($M_1 = N \cdot e_0$) and second order effects caused by the lateral deflection of the elements ($M_2 = N \cdot d$).

Table 4. Summary of key experimental results.

Specimen	N_u [kN]	M_u [kNm]	d_u [mm]	θ_u [rad]	e_0 [mm]	e' [mm]
S1-CC	447.5	2.4	5.5	0.028	0	0.6
S1-EC1	256.0	11.0	23.0	0.104	20	17.3
S1-EC2	193.5	13.4	29.2	0.127	40	34.7
S2-CC	173.1	1.7	9.9	0.044	0	1.4
S2-EC1	79.9	4.9	31.2	0.135	30	29.7
S3-CC	130.2	2.4	18.6	0.078	0	1.1
S3-EC1	76.4	6.0	38.6	0.167	20	22.7
S4-CC	364.5	2.8	6.6	0.034	0	0.8
S4-EC1	222.8	8.2	16.7	0.076	20	17.9
S5-CC	97.4	0.8	8.4	0.032	0	1.2
S5-EC1	62.4	2.3	25.2	0.103	12.5	11.3
S5-EC2	44.3	2.4	28.8	0.123	25	29.4

Nominal load eccentricities e_0 have also been compared to those calculated from strain gauge measurements e' in Table 4. The determination of the experimental load eccentricity has been derived through Eq. (2), where ε_{max} is the measured strain at the maximum compressed fibre and ε_{min} the measured maximum tensile or minimum compressive strain at the other extreme fibre, B is the outer dimension of the element, E is the Young's modulus, I is the relevant second moment of area, d is the lateral deflection at each loading step N and w_0 is the initial imperfection amplitude. Note that the experimental eccentricities provided in Table 4 are the average values of the eccentricities calculated at those loading steps where the material behaved elastically, with a constant Young's modulus. The similarity between e_0 and e' values indicate the reliability of the conducted tests.

$$e^{'} = \frac{EI(\varepsilon_{max} - \varepsilon_{min})}{B \cdot N} - d - w_0 \tag{2}$$

The failure modes observed in the specimens involved overall flexural buckling for every specimen but for S4, which failed by combined overall and local buckling for both compression and combined loading configurations. Figures 8, 9 and 10 show the failure modes of the S3-EC1 and S4-CC specimens, where the influence of local buckling can be clearly appreciated.

Figure 9. Interaction of local and overall flexural buckling of specimen S4-CC.

Figure 8. Overall flexural buckling failure of specimen S3-EC1.

Figure 10. Detailed view of the local failure of specimen S4-EC1.

Full measured experimental curves for all the conducted tests are presented in Figures 11 to 15. The evolution of total bending moment M_{tot} is presented against the applied total axial load, comparing the behaviour for different load eccentricities in each cross-section. Additionally, the first order bending moment due to load eccentricity e_0 has also been plotted ($M_1 = N \cdot e_0$), in order to evaluate the influence of second order effects caused by the lateral deflection of the elements ($M_2 = N \cdot d$), which are shown not to be negligible. Therefore, M_{tot} gathers first and

second order moments, being $M_{tot}=N \cdot (e_0+d)$. Besides, axial compression loads are also presented against the lateral deflections of the elements, measured at the mid-height section.
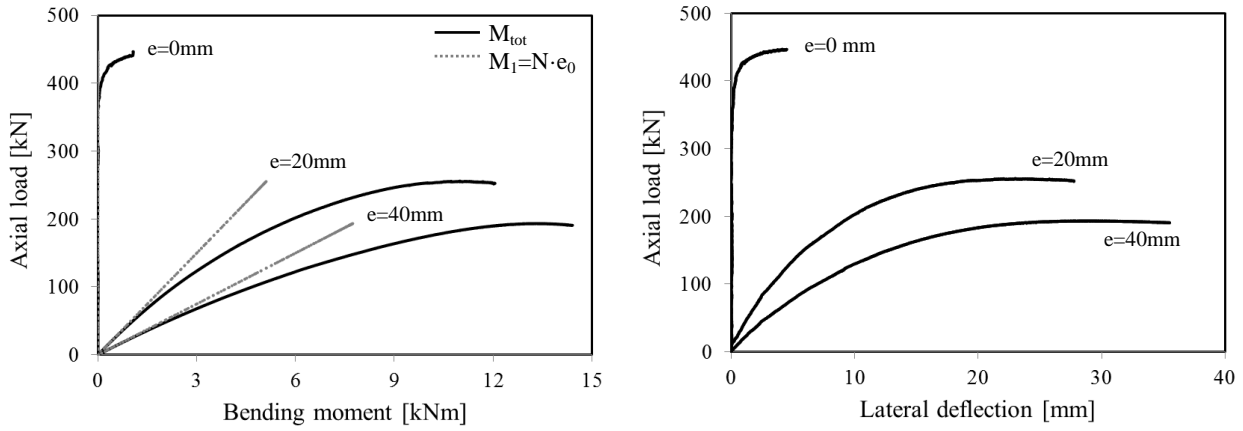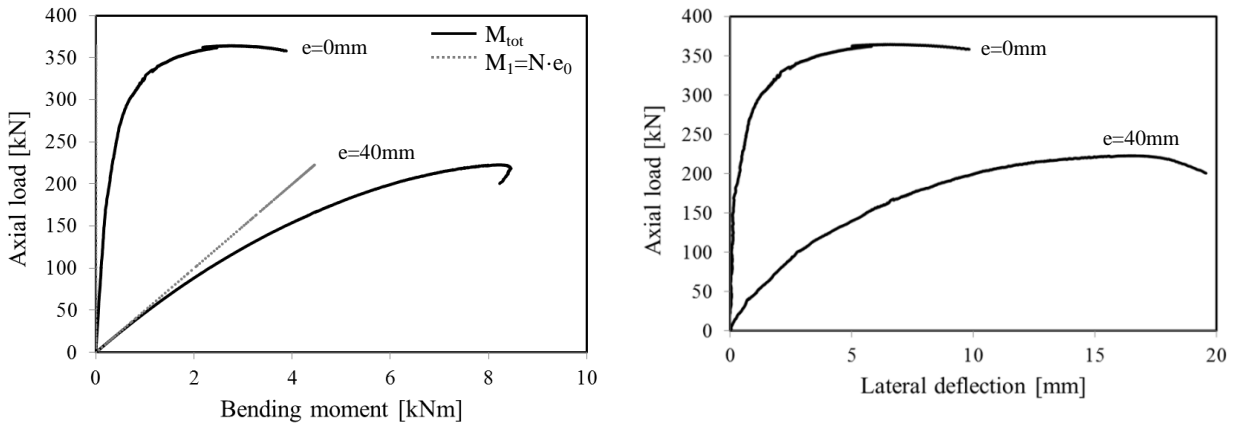

Figure 11. Axial load versus moment and axial load versus lateral deflection curves for S1 specimen.
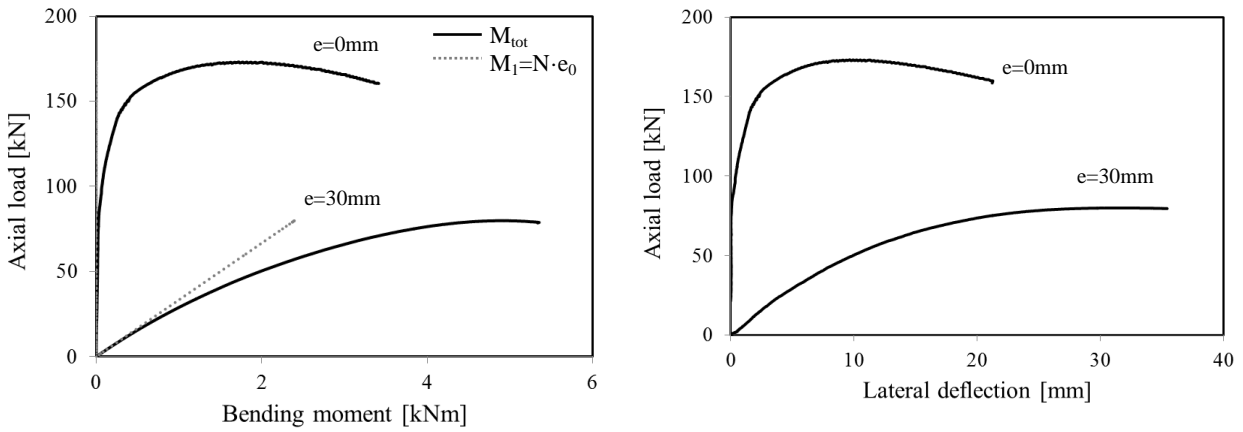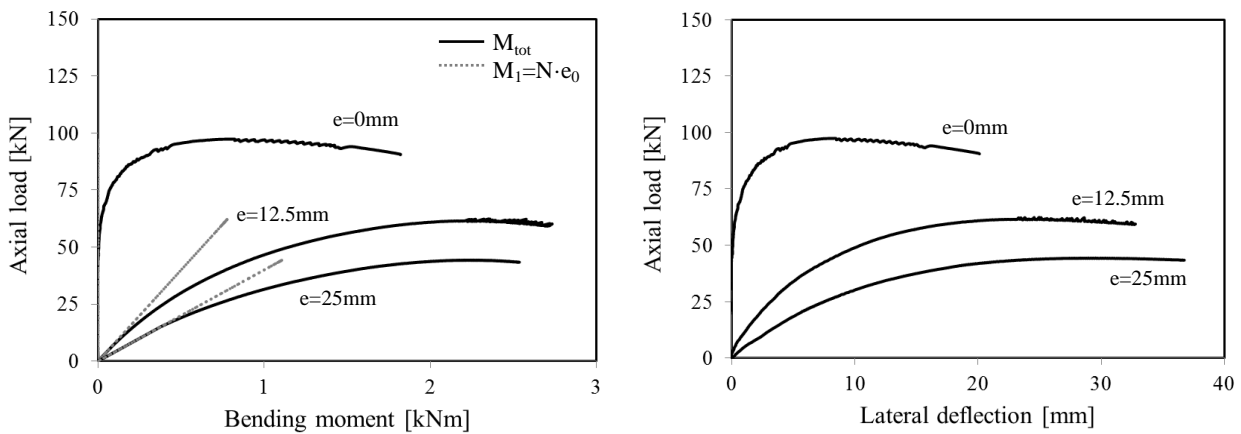

Figure 12. Axial load versus moment and axial load versus lateral deflection curves for S2 specimen.
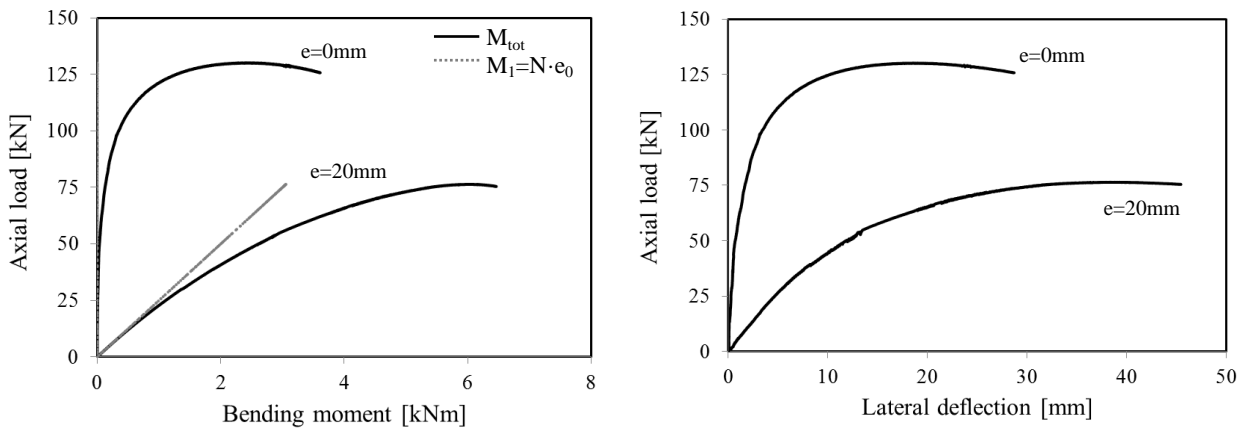
Figure 13. Axial load versus moment and axial load versus lateral deflection curves for S3 specimen.

Figure 14. Axial load versus moment and axial load versus lateral deflection curves for S4 specimen.

Figure 15. Axial load versus moment and axial load versus lateral deflection curves for S5 specimen.

3. DESIGN RULES AND ALTERNATIVE APPROACHES

Different design approaches are available in Standards and the literature for the consideration of flexural buckling and combined loading phenomena. The determination of the ultimate capacity of beam-columns is usually derived through interaction expressions, although the equations for the interaction factor and the calculation of the flexural buckling resistances differ from one to another. A brief description of these expressions is presented in this section, but the complete expressions of each analysed approach are available in the original publications.

3.1 Design expressions for flexural buckling

EN1993-1-4 [1] specifications for the evaluation of the flexural buckling resistance of stainless steel elements subjected to pure compression are based on the Perry-Robertson buckling

15

formulation established in EN1993-1-1 [2] for carbon steel elements, given by Eqs.(3)-(5)

considering $\beta=1$. However, the specific behaviour of stainless steel elements is considered by

adopting different buckling curves and limiting slenderness $\overline{\lambda}_0$ from those codified for similar

carbon steel specimens in order to account for different geometric imperfections and residual

stresses. Regarding stainless steel cold-formed hollow sections, EN1993-1-4 [1] establishes that

the buckling curve c should be considered, with an imperfection factor of $\alpha=0.49$, together with

a limiting slenderness $\overline{\lambda}_0 = 0.4$ for all stainless steel grades.

$$N_{b,Rd} = \frac{\chi A \sigma_{0.2}}{\gamma_{M1}} \tag{3}$$

$$\chi = \frac{1}{\phi + \sqrt{\phi^2 - \beta \overline{\lambda}^2}} \leq 1.0 \tag{4}$$

$$\phi = 0.5 \cdot \left[1 + \alpha(\overline{\lambda} - \overline{\lambda}_0) + \beta \overline{\lambda}^2\right] \tag{5}$$

where A is the cross-sectional area (for Class 4 slender sections, the effective area is used), $\sigma_{0.2}$

is the 0.2% proof stress and γ_{M1} is the instability partial safety factor.

In opposition, SEI/ASCE-8 [7] considers the nonlinear stress-strain response of the material by

allowing a gradual yielding through the use of the tangent modulus E_t corresponding to the

buckling stress into flexural buckling resistance calculations. AS/NZS [8] does also consider an

iterative design procedure in addition to an explicit design procedure, which is essentially the

method codified in EN1993-1-4 [1] but considering a nonlinear expression for the imperfection

parameter, described by Eqs. (6)-(9), with six different buckling curves for different stainless

steel grades. For the ferritic grade analysed in this paper, $\alpha=0.94$, $\beta=0.15$, $\lambda_0=0.56$ and $\lambda_1=0.27$

parameter values are provided.

$$N_{b,Rd} = \phi_c A F_n \tag{6}$$

$$F_n = \frac{\sigma_{0.2}}{\phi + \sqrt{\phi^2 - \overline{\lambda}^2}} \tag{7}$$

$$\phi = \frac{1}{2} \left[1 + \eta + \overline{\lambda}^2\right] \tag{8}$$

$$\eta = \alpha \left[\left(\bar{\lambda} - \lambda_1 \right)^\beta - \lambda_0 \right] \qquad (9)$$

Alternatively, Lopes et al. [19] proposed the introduction of a β=1.5 factor in Eqs. (3)-(5) for the determination of the reduction factor χ after a numerical study on austenitic stainless steel I columns in order to ensure conservative results.

3.2 Design expressions for beam-columns

Regarding design expressions for the evaluation of stainless steel beam-columns, different approaches can be found in Standards and the literature. Nevertheless, compression and bending moment interaction verifications are usually presented as interaction expressions with the same general expression, given by Eq. (10), and a certain interaction factor *k*. The differences among these expressions basically lay on the definition of this interaction factor *k* and the calculation of the basic flexural buckling $N_{b,Rd}$ and bending moment $M_{c,Rd}$ capacities.

$$\frac{N_{Ed}}{N_{b,Rd}} + k \frac{M_{Ed}}{M_{c,Rk} / \gamma_{M1}} \le 1.0 \qquad (10)$$

The interaction expression codified in EN1993-1-4 [1] is described by Eq. (11), where the minimum value of 1.2 is worth mentioning, which usually derives into overconservative capacity predictions since the full bending capacity of the cross-section cannot be reached for low axial compression values. Other Standards, such as SEI/ASCE-8 [7] and AS/NZS [8], consider an interaction factor *k* given by Eq. (12), where C_m is the equivalent uniform moment factor and N_{cr} is the elastic buckling load.

Several interaction expressions available in the literature consider the shape of the bending moment diagram through the μ parameter, and were based in the proposal published by Lopes et al. [20], which is given by Eq. (13) when A=B=1 are considered. This expression was calibrated for I beam-columns considering different stainless steel grades and bending moment

diagrams and was then recalibrated for stainless steel RHS and SHS elements by Jandera and Syamsuddin [21] with A=B=1.2 and by Arrayago et al. [11] with A=1 and B=0.92.

Greiner and Kettler [22] conducted an extensive numerical analysis of austenitic and duplex stainless steel I, rectangular hollow section and circular hollow section elements subjected to compression and uniform bending diagrams, and proposed a different interaction expression for rectangular hollow sections, given by Eq. (14).

$$k = 1.0 + 2(\bar{\lambda} - 0.5)\frac{N_{Ed}}{N_{b,Rd}} \qquad 1.2 \le k \le 1.2 + 2\frac{N_{Ed}}{N_{b,Rd}} \tag{11}$$

$$k = \frac{C_m}{1 - \dfrac{N_{Ed}}{N_{cr}}} \tag{12}$$

$$k = A - B\frac{\mu N_{Ed}}{N_{b,Rd}} \tag{13}$$

$$k = 0.9 + 3.5\left(\frac{N_{Ed}}{N_{b,Rd}}\right)^{1.8}(\bar{\lambda} - 0.5) \le 0.9 + 1.75\left(\frac{N_{Ed}}{N_{b,Rd}}\right)^{1.8} \tag{14}$$

4. ASSESSMENT OF DESIGN APPROACHES

The experimental results presented in previous sections have been carefully analysed and used for the assessment of the different existing approaches for the determination of the flexural buckling resistance of ferritic stainless steel RHS and SHS columns and also for the interaction expressions for combined loading. Both Standard-codified and alternative expressions published in the literature have been considered for the evaluation of the best approach. This section investigates the accuracy and applicability of the different expressions by comparing the predicted capacities with those obtained in the experimental tests.

4.1 Assessment of flexural buckling design approaches

The assessment of the expressions presented in the previous section is analysed herein through a comparison of the experimental flexural buckling capacities with the predicted values calculated from the expressions given in EN1993-1-4 [1], SEI/ASCE-8 [7], AS/NZS [8] and

Lopes et al. [19]. Note that the instability partial safety factor γ_{M1} and the resistance factors ϕ have been set to unity for comparison and the weighted average material properties presented in Table 2 have been considered. Table 5 presents the assessment of the different expressions for the calculation of the flexural buckling resistance by analysing the predicted to experimental load ratios. Mean values and the coefficients of variation (COV.) are also presented, together with the element slenderness of each tested specimen, calculated according to Eq. (1).

Table 5. Assessment of different approaches for flexural buckling resistance considering weighted material properties.

Specimen	$\bar{\lambda}$	$N_{b,EN}/N_{b,exp}$	$N_{b,ASCE}/N_{b,exp}$	$N_{b,AS/NZS}/N_{b,exp}$	$N_{b,Lopes}/N_{b,exp}$
S1-CC	0.93	0.87	1.01	0.79	0.73
S2-CC	1.13	0.90	1.23	0.89	0.72
S3-CC	1.72	0.86	1.11	0.92	0.63
S4-CC	0.65	0.85	0.84	0.72	0.81
S5-CC	1.20	0.89	1.20	0.88	0.69
	Mean	0.87	1.08	0.84	0.72
	COV.	0.024	0.147	0.096	0.091

Table 5 demonstrates that overall, the estimation of the flexural buckling resistance of ferritic stainless steel columns is good for the considered expressions, although SEI/ASCE-8 [7] specifications seem to overpredict ultimate loads for most elements. In general, the buckling curve currently codified in EN1993-1-4 [1] seems to be the most appropriate one for the evaluation of the flexural buckling capacity of ferritic stainless steel RHS and SHS elements, although the specific curve proposed for grade EN1.4003 in AS/NZS [8] also provides good results.

In Figure 16, reduction factors χ have been calculated by normalizing the experimental ultimate loads with the corresponding squash loads and have been plotted against the relative slenderness. Stub column test results reported in [13] have also been included in this analysis, together with the different buckling curves analysed in this section.
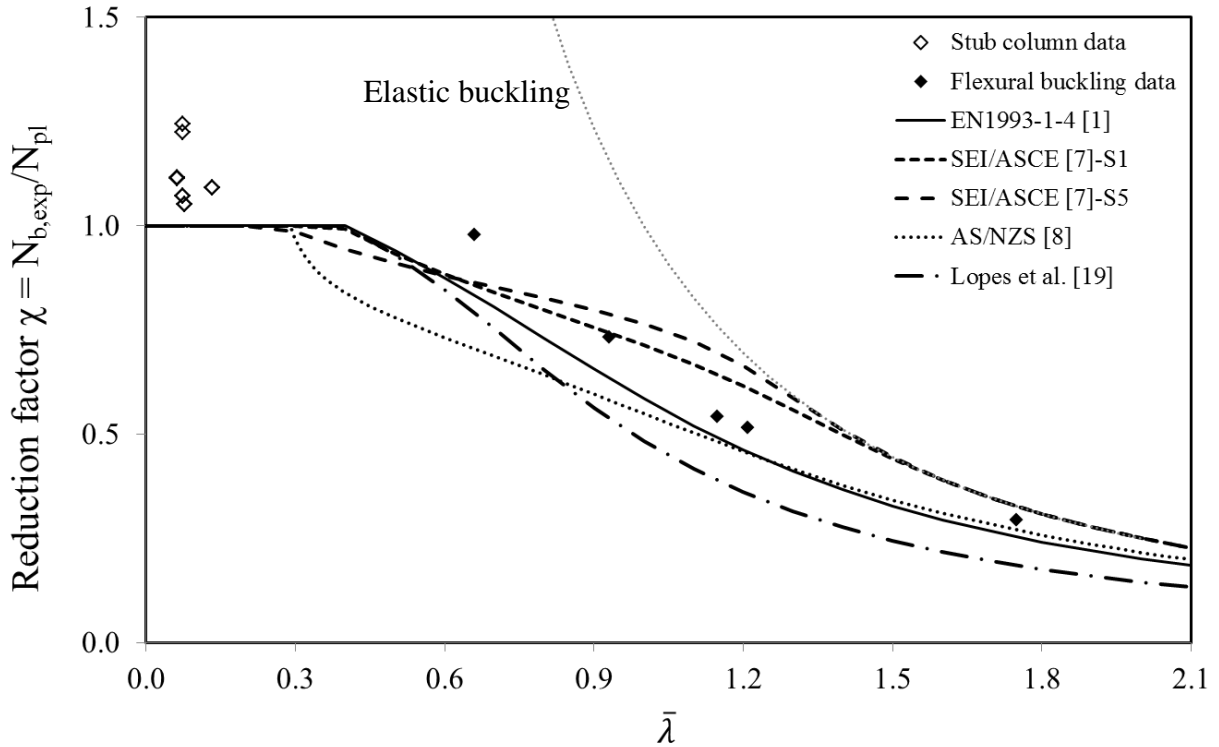
Figure 16. Flexural buckling test results and design approach comparison.

Since Figure 16 demonstrates, the buckling curve codified in EN1993-1-4 [1] for stainless steel hollow elements presents the best estimation of the flexural buckling behaviour of ferritic RHS and SHS columns. The AS/NZS [8] buckling curve lays below the EN1993-1-4 curve, and hence, the ultimate capacity predictions are slightly more conservative but still safe. However, since the curves codified in SEI/ASCE-8 [7] are, as shown in Figure 16, the highest ones for the slenderness values involved in the study, experimental results are usually overpredicted.

The experimental results and conclusions reported in [6] for ferritic stainless steel RHS and SHS found some unsafe flexural buckling load predictions for $\bar{\lambda}$ slenderness values around 0.8-1.0. A column with a 60x60x3 cross-section and L=1577mm was also tested, equivalent to the specimen S2-CC tested in the experimental programme presented in this paper. An ultimate load of 166kN was obtained in the tests reported in [6], which does not differ more than 4% from the 173kN result presented in Table 4. The main difference between both specimens is the measured real geometry, initial imperfection and the material characterization, making the

predicted ultimate loads slightly different and therefore obtaining unsafe results. Thus, as the behaviour for higher and lower slenderness is similar in both experimental programmes, the buckling curve currently codified in EN1993-1-4 [1] seems to be adequate for the slenderness analysed in this paper but could be, as [6] reports, unsafe for some other cases. Nevertheless, as the number of available flexural buckling tests on RHS ferritic elements might still be too low to derive a comprehensive statistical evaluation of the partial safety factor, some future experimental and numerical investigations should be conducted.

4.2 Assessment of beam-column design approaches

After the approaches for the prediction of the flexural buckling resistance of ferritic RHS and SHS columns have been investigated, the interaction expressions for beam-column elements need to be assessed. The different approaches described in section 3.2 have been considered in this analysis in order to evaluate their applicability and accuracy regarding ferritic stainless steel elements.

For the evaluation of these interaction expressions, the same procedure followed by [11],[13] has been adopted, where U ratios by which each experimental data point exceeds or falls short of its respective design interaction curve have been calculated assuming proportional loading, as defined in Eq. (15) and Figure 17. Note that U values greater than unity indicate unsafe predictions of ultimate capacities. For the determination of the applied bending moment, the calculated eccentricities e' reported in Table 4 have been considered.

$$U = R_{pred} / R_{exp}$$
(15)
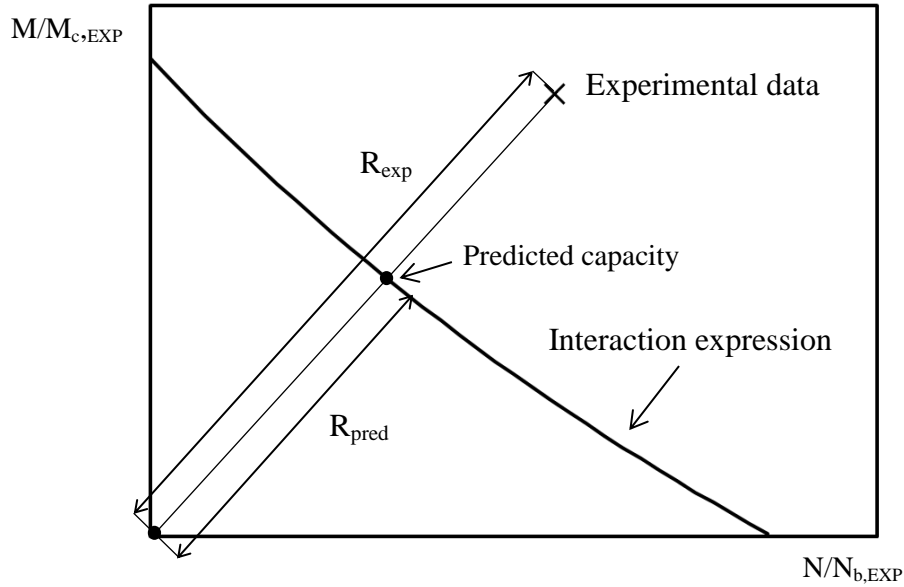
Figure 17. Graphic definition of U parameter for the assessment of design approaches.

It is important to note that the accuracy of these interaction approaches is inherently dependent on the correct flexural buckling $N_{b,Rk}$ and bending moment $M_{c,Rk}$ resistance determination. Therefore, the assessment of the different expressions has been investigated by using both the predicted $N_{b,Rk}$ and $M_{c,Rk}$ resistances and those determined from experimental tests. Flexural buckling resistances of the different elements have already been presented in this paper, while experimental bending moment resistances used in this study are those reported in [12]. Although the experimental programme was described in the original paper, the most relevant tests results of the conducted four-point bending tests on specimens with the same cross-section are gathered in Table 6. F_u is the ultimate load, d_u is the corresponding midspan deflection and M_u is the reached ultimate bending moment. The comparison of the bending capacities against elastic (M_{el}) and plastic (M_{pl}) bending moment capacities is also presented.

Table 6. Summary of key experimental results for simply supported beams in [12].

Section	F_u [kN]	d_u [mm]	M_u [kNm]	M_u/M_{el}	M_u/M_{pl}
S1	66.1	42.4	16.9	1.18	0.96
S2	27.2	59.6	6.9	1.23	1.00
S3-Mj	43.2	63.8	11.0	1.36	1.02
S3-Mi	26.3	104.4	6.7	1.26	1.01
S4-Mj	64.1	16.3	16.3	1.03	0.84
S4-Mi	48.6	22.5	12.4	0.97	0.83

S5-Mj	19.2	48.0	4.9	1.26	1.03
S5-Mi	13.9	49.9	3.5	1.09	0.94

Table 7 gathers the U ratios calculated for each tested specimen and each design approach when the calculated flexural buckling and bending moment resistances are considered. Note that besides being different interaction expressions, they also consider different expressions for the determination of $N_{b,Rk}$ and $M_{c,Rk}$. In contrast, Table 8 presents similar results, but based on the experimentally determined flexural buckling and bending moment resistances.

Table 7. Assessment of beam-column design approaches considering calculated resistances.
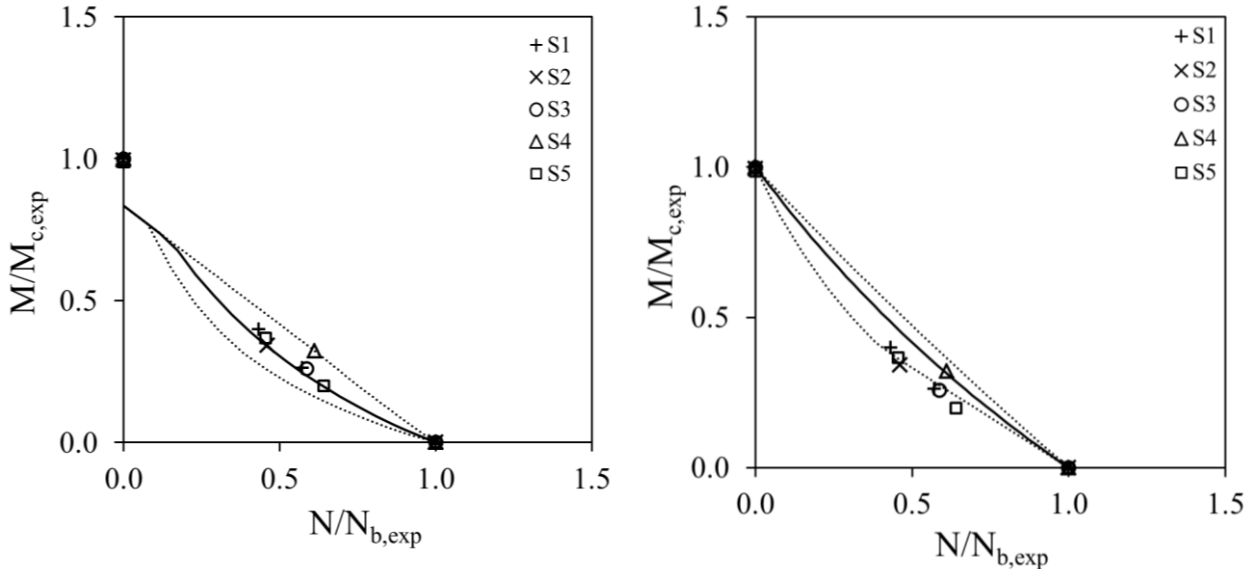
Specimen	EN1993-1-4 [1]	Lopes et al. [20]	Jandera and Syamsuddin [21]	Arrayago et al. [11]	Greiner and Kettler [22]	SEI/ASCE [7]	AS/NZS [8]
S1-EC1	0.89	0.95	0.89	0.96	0.89	0.96	0.85
S1-EC2	0.80	0.94	0.86	0.95	0.91	0.94	0.86
S2-EC1	0.88	1.01	0.93	1.02	0.98	1.08	0.95
S3-EC1	0.72	0.81	0.76	0.82	0.85	0.89	0.83
S4-EC1	0.81	0.89	0.83	0.89	0.86	0.85	0.75
S5-EC1	0.83	0.92	0.87	0.92	0.87	1.02	0.86
S5-EC2	0.77	0.89	0.82	0.90	0.89	0.97	0.86
Mean	0.82	0.92	0.85	0.92	0.89	0.96	0.85
COV.	0.073	0.068	0.066	0.067	0.049	0.079	0.069

Table 8. Assessment of beam-column design approaches considering experimental resistances.

Specimen	EN1993-1-4 [1]	Lopes et al. [20]	Jandera and Syamsuddin [21]	Arrayago et al. [11]	Greiner and Kettler [22]	SEI/ASCE [7]	AS/NZS [8]
S1-EC1	1.03	1.11	1.04	1.12	1.04	1.01	1.01
S1-EC2	1.02	1.10	1.01	1.11	1.06	1.02	1.02
S2-EC1	0.99	1.10	1.01	1.11	1.07	1.02	1.02
S3-EC1	0.86	0.97	0.91	0.98	1.01	0.92	0.92
S4-EC1	1.00	1.05	0.98	1.05	1.02	0.96	0.96
S5-EC1	0.98	1.07	1.01	1.08	1.02	0.98	0.98
S5-EC2	0.95	1.06	0.97	1.07	1.05	0.99	0.99
Mean	0.98	1.07	0.99	1.07	1.04	0.99	0.99
COV.	0.058	0.045	0.044	0.044	0.023	0.037	0.037

The assessment of the interaction expressions presented in Table 7 shows that all design approaches provide safe and quite accurate results regarding ferritic stainless steel RHS and SHS beam-elements when uniform bending moment distributions are considered. The design

23

approaches that better predict the ultimate capacity of the tested specimens with the lowest scatter are, nevertheless, the expression proposed by Lopes et al. [20] and Arrayago et al. [11] together with codified expression in SEI/ASCE [7]. However, when experimental $N_{b,exp}$ and $M_{c,exp}$ capacities are considered, the interaction expressions codified in the different Standards provide excellent ultimate capacity predictions, as mean U ratios shown in Table 8 are very close to unity. Note that when experimental resistances are considered in Table 8, as the interaction expressions codified in SEI/ASCE-8 [7] and AS/NZS [8] are the same, equal assessment ratios are obtained. Regarding the alternative methods proposed in the literature, a slight overestimation can be appreciated when experimental flexural buckling and bending moment resistances are considered.

Figure 18 presents same results graphically, comparing the interaction curves with the experimental results in a normalized axial compression-bending moment space in order to facilitate comparison between different cross-sections. Although each analysed cross-section presents a different interaction expression for each approach, only the highest, lowest and average interaction curves have been plotted for simplicity, and both interaction curves and experimental data have been normalized with the corresponding experimental resistances.
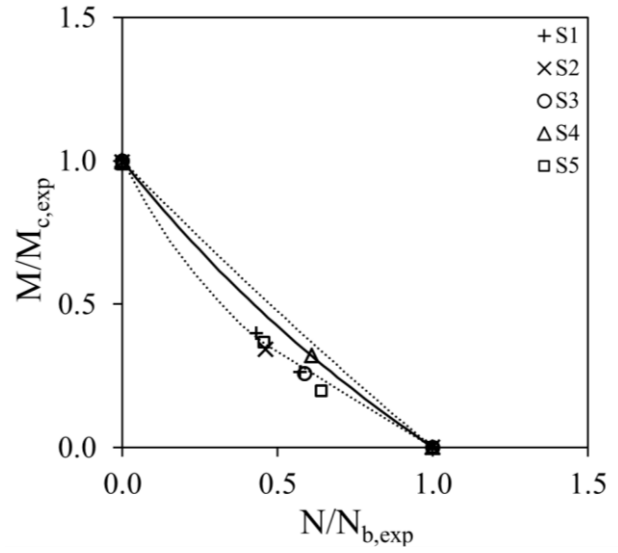

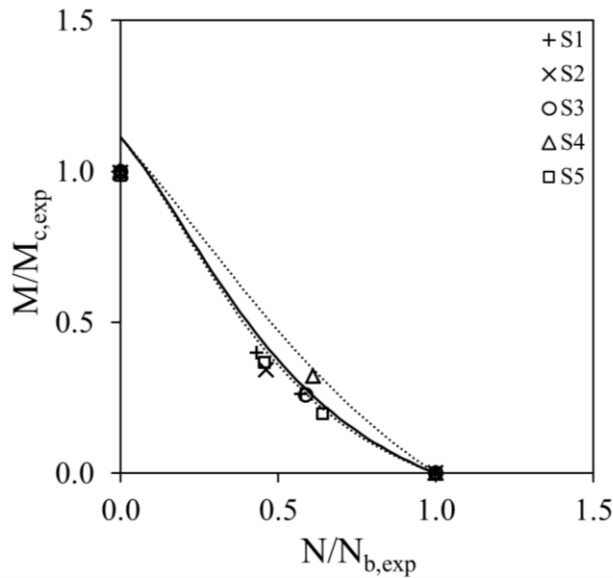a) Assessment of EN1993-1-4 [1] interaction approach.

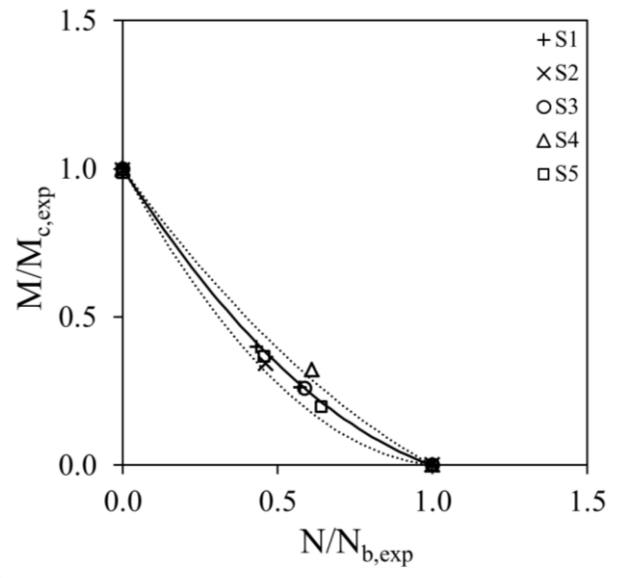b) Assessment of Lopes et al. [20] interaction approach.
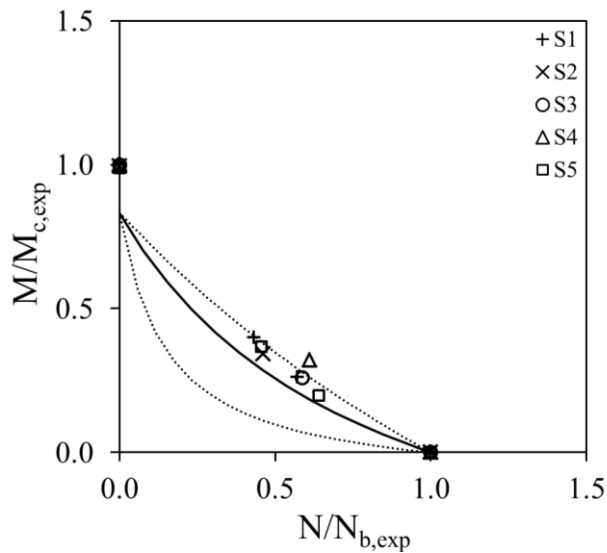
c) Assessment of Jandera and Syamsuddin [21] interaction approach.

d) Assessment of Arrayago et al. [11] interaction approach.

e) Assessment of Greiner and Kettler [22] interaction approach.

f) Assessment of SEI/ASCE-8 [7] and AS/NZS [8] interaction approaches.

Figure 18. Assessment of interaction approaches for beam-columns.

4.3 Statistical analysis: resulting γ_{M1} partial safety factors

This final section gathers the statistical analysis of the obtained results regarding flexural buckling and combined loading design approaches. The authors are aware about the limited experimental data analysed in this paper and the statistical analysis presented does not aim to be a reliability analysis of the mentioned approaches as much as a study of the results and a

comparison with the observations reported by Afshan et al. [9] regarding the partial safety factor γ_{M1} for ferritic RHS elements.

The statistical analysis presented herein has been derived according to EN1990, Annex D [10] specifications. Since the steps to be followed and the coefficients have been extensively described in Tankova et al. [23], a summary of the parameter values will be presented herein. The adopted values for the variation of geometric and material properties are those recommended in [9] for ferritic stainless steel. Table 9 presents the summary of the more relevant parameters of the statistical analysis of the approaches for flexural buckling and beam-columns analysed in this paper, where b is the mean value of the correction factor, V_δ is the coefficient of variation of the errors of each approach relative to the experimental results and V_r is the combined coefficient of variation.

Table 9. Summary of the parameters for the statistical analysis of flexural buckling and beam-column approaches.

	Approach	b	V_δ	γ_{M1}
Flexural buckling	EN1993-1-4 [1]	1.159	0.019	1.00
	SEI/ASCE [7]	0.994	0.091	1.08
	AS/NZS [8]	1.271	0.056	0.89
	Lopes et al. [19]	1.327	0.057	0.91
Beam-columns	EN1993-1-4 [1]	1.188	0.052	1.01
	Lopes et al. [20]	1.093	0.043	1.12
	Jandera and Syamsuddin [21]	1.177	0.039	0.99
	Arrayago et al. [11]	1.086	0.041	1.07
	Greiner and Kettler [22]	1.124	0.033	1.03
	SEI/ASCE [7]	1.056	0.047	1.17
	AS/NZS [8]	1.184	0.049	1.04

According to the results gathered in Table 9 regarding flexural buckling behaviour for ferritic stainless steel RHS, all approaches can be safely applied if the partial safety factor γ_{M1} currently codified in EN1993-1-4 [1] is considered, since calculated values are below 1.10. Low γ_{M1} values obtained for AS/NZS [8] and Lopes et al. [19] approaches are due to the high b values

shown in Table 9 and the low average predicted-to-experimental axial load ratios previously presented in Table 5. Regarding beam-column behaviour, Table 9 indicates that most of the studied approaches can be safely applied with the current $\gamma_{M1}=1.10$ value except Lopes et al. [20] and SEI/ASCE [7], probably due to the fact that SEI/ASCE [7] does overestimate the flexural buckling capacity of several cross-sections as shown in Table 5. Summarizing, and although a more extensive analysis based on finite element modelling needs to be derived in order to analyse a bigger database, the available results highlight that the majority of the analysed approaches can be safely applied with the 1.10 safety factor γ_{M1} currently codified in EN1993-1-4 [1] for stainless steel columns and beam-columns.

5. CONCLUSIONS

A comprehensive experimental programme on ferritic stainless steel RHS and SHS columns has been presented in this paper in order to investigate the flexural buckling and beam-column behaviour of these elements. These experimental results are a valuable contribution since the available experimental data on ferritic stainless steel flexural elements is very limited. Twelve specimens comprising five different hollow cross-sections have been tested under pin-ended conditions and with a nominal length of 1500mm. Experimental results allowed for the assessment of the existing design approaches, both for flexural buckling and combined loading, codified in different Standards and proposed in the literature.

Flexural buckling tests demonstrated that the buckling curves currently codified in EN1993-1-4 [1] and AS/NZS [8] provide safe and accurate resistance predictions for the analysed cross-sections, whilst the iterative method specified in SEI/ASCE [7] seems to overpredict flexural capacities. Regarding flexural buckling and bending moment interaction, all design approaches codified in Standards and proposed in the literature have been found to be safe and accurate for the experimental results presented in this paper, considering uniform bending moment

distributions. The preliminary statistical analysis derived from the available data highlighted that the currently codified partial safety factor γ_{M1} can be safely applied for most of the approaches analysed for flexural buckling and beam-columns.

However, a more extensive analysis on combined loading should be conducted in order to extend this analysis to different bending moment diagram shapes through more experimental tests and extensive numerical parametric studies considering several element lengths, cross-sectional shapes and stainless steel grades in order to obtain more general conclusions.

6. ACKNOWLEDGEMENTS

7. REFERENCES

[1] EN1993-1-1. Eurocode 3: design of steel structures – Part 1–1: general rules and rules for building. Brussels: European Committee for Standardization (CEN), 2005.

[2] EN 1993-1-4. Eurocode 3: design of steel structures – Part 1–4: general rules – supplementary rules for stainless steels. Brussels: European Committee for Standardization (CEN), 2006.

[3] Talja A and Salmi P. Design of stainless steel RHS beams, columns and beam-columns. Technical note, VTT Research Centre, Finland. 1995.

[4] Lui WM, Ashraf M and Young B. Tests of cold-formed duplex stainless steel SHS beam-columns. Engineering Structures 74 (2014), 111–121.

[5] Huang Y and Young B. Experimental investigation of cold-formed lean duplex stainless steel beam-columns. Thin-Walled Structures 76 (2014), 105–117.

[6] Afshan S and Gardner L. Experimental study of cold-formed ferritic stainless steel hollow sections. Journal of Structural Engineering, 139 (special issue) (2013), 717–728.

[7] SEI/ASCE 8-02. Specification for the design of cold-formed stainless steel structural members. Reston: American Society of Civil Engineers (ASCE); 2002.

[8] AS/NZS 4673. Cold-formed stainless steel structures. Sydney: Standards Australia; 2001

[9] Afshan S, Francis P, Baddoo NR, Gardner L. Reliability analysis of structural stainless steel design provisions. Journal of Constructional Steel Research 114 (2015), 293–304.

[10] EN 1990. Eurocode: basis of structural design. Brussels: European Committee for Standardization (CEN), 2002.

[11] Arrayago I, Picci F, Mirambell E and Real E. Interaction of bending and axial load for ferritic stainless steel RHS columns. Thin-Walled Structures 91 (2015), 96-107.

[12] Arrayago I and Real E. Experimental study on ferritic stainless steel simply supported and continuous beams. Journal of Constructional Steel Research 119 (2014), 50-62.

[13] Arrayago I and Real E. Experimental study on ferritic stainless steel RHS and SHS cross-sectional resistance under combined loading. Structures 4 (2015), 69-79.

[14] EN ISO 6892-1. Metallic materials - Tensile testing - Part 1: Method of test at room temperature. Brussels: European Committee for Standardization (CEN); 2009.

[15] Real E, Arrayago I, Mirambell E and Westeel R. Comparative study of analytical expressions for the modelling of stainless steel behaviour. Thin-Walled Structures 83 (2014), 2-11.

[16] Arrayago I, Real E and Gardner L. Material modelling of stainless steel alloys. Materials and Design 87 (2015), 540–552.

[17] Mirambell E and Real E. On the calculation of deflections in structural stainless steel beams: an experimental and numerical investigation. Journal of Constructional Steel Research, 54(1) (2000), 109–133.

[18] Hradil P and Talja A. Investigating the role of gradual yielding in stainless steel columns and beams by virtual testing. Proceedings of The Fifth International Conference on Structural Engineering, Mechanics and Computation. Cape Town, South Africa (2013), 1459–1464.

[19] Lopes N, Vila Real P and Simões da Silva L. Numerical modelling of the flexural buckling of axially loaded stainless steel members. Proceedings of the Third International Conference on Steel and Composite Structures ICSCS07, Manchester, United Kingdom, 2007.

[20] Lopes N, Vila Real P and Simões da Silva L. Stainless steel beam-columns interaction curves with and without lateral torsional buckling. 7th EUROMECH Solid Mechanics Conference, Lisbon, 2009.

[21] Jandera M and Syamsuddin D. Interaction formula for stainless steel beam-columns. Recent research advances on thin-walled structures, 2014. Proceedings of the Seventh European Conference on Steel and Composite Structures (EUROSTEEL), Napoli (Italy), 10-12 September 2014.

[22] Greiner R and Kettler M. Interaction of bending and axial compression of stainless steel members. Journal of Constructional Steel Research, 64(11) (2008), 1217–1224.

[23] Tankova T, Simoes da Silva L, Marques L, Rebelo C and Taras A. Towards a standardized procedure for the safety assessment of stability design rules. Journal of Constructional Steel Research 103 (2014), 290-302.